

Finite-size scaling functions for directed polymers confined between attracting walls

This article has been downloaded from IOPscience. Please scroll down to see the full text article.

2008 J. Phys. A: Math. Theor. 41 035002

(<http://iopscience.iop.org/1751-8121/41/3/035002>)

View [the table of contents for this issue](#), or go to the [journal homepage](#) for more

Download details:

IP Address: 171.66.16.149

The article was downloaded on 03/06/2010 at 07:00

Please note that [terms and conditions apply](#).

Finite-size scaling functions for directed polymers confined between attracting walls

A L Owczarek¹, T Prellberg² and A Rechnitzer³

¹ Department of Mathematics and Statistics, The University of Melbourne, Parkville, Victoria 3052, Australia

² School of Mathematical Sciences, Queen Mary, University of London, Mile End Road, London E1 4NS, UK

³ Department of Mathematics, University of British Columbia, Vancouver, BC V6T 1Z2, Canada

E-mail: aleks@ms.unimelb.edu.au, t.prellberg@qmul.ac.uk and andrewr@math.ubc.ca

Received 20 September 2007, in final form 19 November 2007

Published 4 January 2008

Online at stacks.iop.org/JPhysA/41/035002

Abstract

The exact solution of directed self-avoiding walks confined to a slit of finite width and interacting with the walls of the slit via an attractive potential has been recently calculated. The walks can be considered to model the polymer-induced steric stabilization and sensitized flocculation of colloidal dispersions. The large-width asymptotics led to a phase diagram different to that of a polymer attached to, and attracted to, a single wall. The question that arises is: Can one interpolate between the single wall and two wall cases? In this paper, we calculate the *exact* scaling functions for the partition function by considering the two variable asymptotics of the partition function for simultaneous large length and large width. Consequently, we find the scaling functions for the force induced by the polymer on the walls. We find that these scaling functions are given by elliptic ϑ functions. In some parts of the phase diagram there is more a complex crossover between the single wall and two wall cases and we elucidate how this happens.

PACS numbers: 05.50.+q, 05.70.fh, 61.41.+e

(Some figures in this article are in colour only in the electronic version)

1. Introduction

The problem of a single polymer confined between two walls and interacting with those walls has been considered for at least 35 years [1]. One reason for this is its use as a model of the stabilization of colloidal dispersions by adsorbed polymers (steric stabilization) and the destabilization when the polymer can adsorb on surfaces of different colloidal particles (sensitized flocculation). Until recently, even when one substitutes directed walks for the

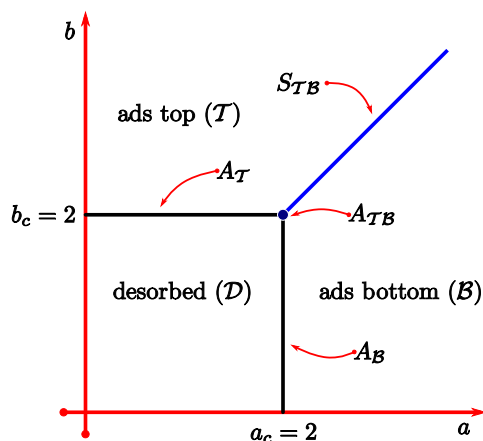


Figure 1. Phase diagram of the infinite strip where the separation of the walls is made large after the limit of infinite walk length is taken. There are three phases: desorbed (des), adsorbed onto the bottom wall (ads bottom) and adsorbed onto the top (ads top). Our notation for the various regions and transition lines are marked. The transition lines at $a = 2, b \leq 2$ and $b = 2, a \leq 2$ marking the boundary of the desorbed region are second-order phase transitions with a jump in the specific heat on crossing the line while the line marking the boundary at $a = b, a > 2$ of the two adsorbed regions is a first-order transition.

more canonical self-avoiding walks in a two-dimensional lattice model of this phenomenon, the only cases to be considered exactly have been special cases where the interaction with the two surfaces are equal. Recently, Brak *et al* [2] have calculated the generating functions for a directed self-avoiding walk confined by two horizontal walls on the square lattice where separate Boltzmann weights a and b were associated with visits to the lower wall and upper wall, respectively, with various restrictions on the end points of the walks.

The dominant singularity of the generating function of any of the subcases considered by Brak *et al* [2] leads to the calculation of the free energy and the force induced by the polymer to the walls. By considering the dominant singularity one is effectively considering the infinite walk length limit. The dominant singularities of the generating functions were analysed asymptotically for large widths. In the infinite width limit a novel phase diagram was obtained, different to the one obtained by analysing a polymer in a half-plane geometry. In figure 1 the phase diagram obtained by Brak *et al* [2] is given. For small a and b the polymer is desorbed from both walls while for large a , respectively large b , the polymer is adsorbed onto one wall or the other. It is interesting to note that new numerical results [3, 4] and rigorous results [5] show that undirected self-avoiding walks demonstrate very similar behaviour to the exact solution of the directed walk model. In the infinite width limit, referred to as the *infinite slit* (in two dimensions), the (reduced) free energy $\kappa(a, b)$ is given by

$$\kappa^{is}(a, b) = \begin{cases} \log(2) & a, b \leq 2 \\ \log\left(\frac{a}{\sqrt{a-1}}\right) & a > 2 \quad \text{and} \quad a > b \\ \log\left(\frac{b}{\sqrt{b-1}}\right) & b > 2 \quad \text{and} \quad a < b. \end{cases} \quad (1.1)$$

In the half-plane geometry, the limit of infinite wall separation is effectively taken before the limit of infinite walk length (see figure 2). The results in [2] imply, unusually, that the

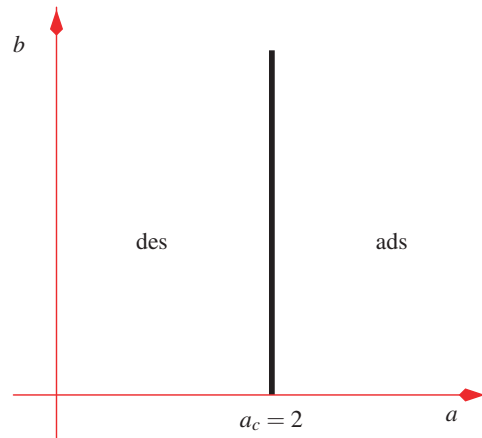


Figure 2. Phase diagram of the half-plane (one wall) problem where the separation of the walls is made large *before* the limit of infinite walk length is taken. There are two phases: desorbed (des) and adsorbed onto the bottom wall (ads bottom). The boundary of the two phase is a second-order phase transition.

order of the two limits, polymer length to infinity and wall separation to infinity, are not interchangeable. In fact, the free energy depends only upon the value of a and is given by

$$\kappa^{hp}(a, b) = \begin{cases} \log(2) & a \leq 2 \\ \log\left(\frac{a}{\sqrt{a-1}}\right) & a > 2. \end{cases} \quad (1.2)$$

Hence, for $b > 2$ and $a < b$ (denoted region \mathcal{T} in figure 1), the infinite-slit and half-plane free energies are different. The question that naturally arises is whether there is a scaling function that interpolates between these two limits and whether this extends to the region where the free energies differ. To do this one needs to consider the finite length partition functions rather than the generating functions. An exact expression for the finite length partition function has now been calculated [6]. However, it is not easy to see how one could analyse this expression asymptotically, especially for large separations. Returning to the undirected model, in three dimensions, a scaling theory [4] valid for the desorbed region \mathcal{D} of the infinite slit and its boundaries has been shown (numerically) to hold.

In this paper, we calculate the two variable asymptotics for large wall separation and large polymer length of the partition function of one of the directed walk models considered by Brak *et al* [2]. The paper is set out as follows. In section 2, we set the stage for our calculations: we recall the exact definition of the model and the calculated generating function, and introduce the notation which we will use in the remainder of the paper, in particular, a parametrization in more convenient variables. Much of the analysis hinges on the understanding of the singularities of the generating function; this will be discussed in section 3. In section 4, we show how the contour integral expression for the partition function can be reformulated in terms of residues of the singularities of the generating function. We discuss special cases for specific values of a and b , where one obtains simple expressions for the partition function, and also give an exact expression for general a and b . In section 5, we calculate the scaling function of the partition function for the special cases, and then derive the scaling function in the various regions of the phase diagram for general a and b . In section 6, we discuss the results in the light of finite size scaling theory and, in particular, discuss how in each region of the phase diagram the scaling results interpolate between the single and double wall

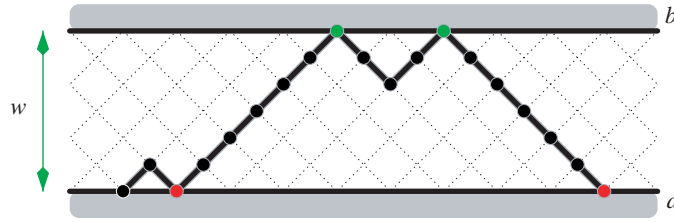


Figure 3. An example of a directed path which is a loop: both ends of the walk are fixed to be on the bottom wall. A Boltzmann weight a is associated with visits to the bottom wall (excluding the first) and a Boltzmann weight b is associated with visits to the top wall.

models. Importantly, we demonstrate that in the desorbed region of the infinite slit and on its boundaries the scaling theory proposed for undirected SAW in a three-dimensional slab holds exactly for our directed model, with appropriate exponent substitutions.

2. The model

Brak *et al* [2] considered three different end-point restrictions. In this paper, we shall restrict ourselves to the case when both end points are attached to the same wall: in [2] these were referred to as *loops* (see figure 3). If \mathcal{L}_w^n is the set of loops of fixed-length n edges in the slit of width w then the partition function of loops is defined as

$$Z_{n,w}(a, b) = \sum_{p \in \mathcal{L}_w^n} a^{u(p)} b^{v(p)}, \tag{2.1}$$

where $u(p)$ and $v(p)$ are the number of vertices in the line $y = 0$ (excluding the zeroth vertex) and the number of vertices in the line $y = w$, respectively. The generating function $L_w(z, a, b)$ is then given by

$$L_w(z, a, b) = \sum_{n=0}^{\infty} Z_{n,w}(a, b) z^n. \tag{2.2}$$

The force $\mathcal{F}_{n,w}(a, b)$ is defined as

$$\mathcal{F}_{n,w}(a, b) = \frac{\log(Z_{n,w+1}(a, b)) - \log(Z_{n,w}(a, b))}{n} \tag{2.3}$$

but can be estimated from an asymptotic expression for large w as

$$\mathcal{F}_{n,w} = \frac{1}{n Z_{n,w}} \frac{\partial Z_{n,w}}{\partial w}. \tag{2.4}$$

The aim of this paper is to extract the asymptotics of the finite size partition function $Z_{n,w}(a, b)$ by inverting equation (2.2). Hence we have

$$Z_{n,w}(a, b) = \frac{1}{2\pi i} \oint L_w(z, a, b) \frac{dz}{z^{n+1}}, \tag{2.5}$$

where the generating function $L_w(z, a, b)$ has been calculated in [2] and is

$$L_w(z, a, b) = \frac{(1+q)[(1+q-bq) - (1+q-b)q^w]}{(1+q-aq)(1+q-bq) - (1+q-a)(1+q-b)q^w}, \tag{2.6}$$

with $z = \sqrt{q}/(1+q)$. The problem is to evaluate the above contour integral for large but finite n and w .

Before we enter the calculations let us introduce some notation to keep track of the different regions and transitions in the phase diagram of the infinite slit (figure 1). We restrict our discussion to $a, b \geq 1$ and label the *desorbed* region, $a < 2, b < 2$ as \mathcal{D} , the region where the polymer *adsorbs onto the bottom wall*, $a > 2, a > b$ as \mathcal{B} , and the region where the polymer *adsorbs onto the top wall*, $b > 2, b > a$ as \mathcal{T} . The boundary where the region \mathcal{D} meets region \mathcal{B} , $a = 2, b < 2$, that is, when the polymer is critically adsorbing onto the bottom wall, we denote as A_B . The boundary where the region \mathcal{D} meets region \mathcal{T} , $b = 2, a < 2$, that is, when the polymer is critically adsorbing onto the top wall, we denote as A_T . The boundary where the region \mathcal{B} meets region \mathcal{T} , $a = b, a > 2$, that is, when the polymer is equally adsorbed onto the both walls, we denote as S_{TB} . Finally, the point where all three regions and all three lines meet at $a = b = 2$ is denoted A_{TB} .

Mathematically, it is advantageous to re-parametrize L_w by introducing $a = 1 + \lambda^2, b = 1 + \mu^2$ with $\lambda, \mu \geq 0$ and $q = p^2$. Hence $z = p/(1 + p^2)$. In what follows, we will thus work with

$$L_w(z, a, b) = \mathcal{L}_w(p, \lambda, \mu) = \frac{(1 + p^2)[(1 - \mu^2 p^2) + (\mu^2 - p^2)p^{2w}]}{(1 - \lambda^2 p^2)(1 - \mu^2 p^2) - (\lambda^2 - p^2)(\mu^2 - p^2)p^{2w}}, \quad (2.7)$$

so that equation (2.5) becomes

$$Z_{n,w}(a, b) = \frac{1}{2\pi i} \oint \mathcal{L}_w(p, \lambda, \mu)(1 - p^2)(1 + p^2)^{n-1} \frac{dp}{p^{n+1}}. \quad (2.8)$$

3. Singularities

Of crucial importance for the understanding of the structure of the generating function are its singularities, i.e. the zeros of the denominator polynomial

$$D_w(p) = (1 - \lambda^2 p^2)(1 - \mu^2 p^2) - (\lambda^2 - p^2)(\mu^2 - p^2)p^{2w}. \quad (3.1)$$

It is convenient to look at some special cases first, where $D_w(p)$ simplifies considerably. We have

$$D_w(p) = \begin{cases} 1 - p^{4+2w} & \text{for } \lambda = 0, \mu = 0, \\ (1 - p^2)(1 + p^{2+2w}) & \text{for } \lambda = 0, \mu = 1 \text{ or } \lambda = 1, \mu = 0, \\ (1 - \lambda^2 p^2)(1 - \lambda^{-2} p^2)(1 - p^{2w}) & \text{for } \lambda\mu = 1. \end{cases} \quad (3.2)$$

For these special cases, all zeros are simple with the exception of the case $\lambda = 1$ and $\mu = 1$, in which case $p = \pm 1$ is a multiple zero. For general values of λ and μ , we have the following result on the multiplicity of zeros.

Lemma 1. *If $(\lambda, \mu) \neq (1, 1)$, the polynomial*

$$D_w(p) = (1 - \lambda^2 p^2)(1 - \mu^2 p^2) - (\lambda^2 - p^2)(\mu^2 - p^2)p^{2w} \quad (3.3)$$

has simple zeros except possibly at $p = \pm 1$ for a single value of w .

Proof. The polynomial $D_w(p)$ is simply related to the polynomials, $P_w(z)$, defined in [2] as

$$\begin{aligned} P_1(z) &= 1 - abz^2, \\ P_2(z) &= 1 - (a + b)z^2, \\ P_w(z) &= P_{w-1}(z) - z^2 P_{w-2}(z) \quad \text{for } w \geq 3. \end{aligned} \quad (3.4)$$

In particular,

$$D_w(p) = (1 - p^2)(1 + p^2)^{w+1} P_w \left(\frac{p}{1 + p^2} \right). \tag{3.5}$$

We have that $P_w(z)$ is a polynomial of degree $w + 1$ in z , so the expression is indeed polynomial in p . Given equation (3.5), the zeros, p_i , of $D_w(p)$ are therefore either $p = \pm 1$ or images of the zeros, z_i , of $P_w(z)$ given by

$$p = \frac{1 \pm \sqrt{1 - 4z_i^2}}{2z_i}. \tag{3.6}$$

Now, $P_w(z)$ can be related directly to Chebyshev polynomials, which are orthogonal polynomials, as

$$P_w(z) = z^{w-1} \left[(1 - abz^2)U_{w-1} \left(\frac{1}{2z} \right) + (ab - a - b)zU_{w-2} \left(\frac{1}{2z} \right) \right]. \tag{3.7}$$

Moreover, making the transformation to polynomials $Q_w(y)$ via

$$P_{w-1}(z) = z^w Q_w \left(\frac{1}{2z} \right) \quad \text{for } w \geq 2, \tag{3.8}$$

one can recognize that the $Q_w(y)$ are a finite (order 3) perturbation of Chebyshev polynomials [7]. Furthermore, the scaled polynomials $q_n(y) = Q_n(y/2)$ are monic and satisfy the assumptions of Favard’s theorem [8] which gives the existence of a measure on which these polynomials are orthogonal. One can explicitly calculate the measure using a result by Geronimus [7] and find that it has support on $[-1, 1]$.

A standard result on orthogonal polynomials (see theorem 5.4.1 in [9] for example) implies that the zeros of $P_w(z)$ are simple. Hence the images of these zeros under the above mapping are simple, except possibly when $z = \pm 1/2$. If $P_w(z)$ has a zero at $z = \pm 1/2$, then it follows that $D_w(p)$ may have multiple zeros at $p = \pm 1$.

We now show that such multiple zeros at $p = \pm 1$ can only occur for a single value of w . The derivative of $D_w(p)$ at $p = \pm 1$ is given by

$$D'_w(\pm 1) = \mp 4(\lambda^2 \mu^2 - 1) \pm 2(\lambda^2 - 1)(\mu^2 - 1)w. \tag{3.9}$$

If $(\lambda, \mu) \neq (1, 1)$ then this derivative is zero when

$$w = 2 \frac{\lambda^2 \mu^2 - 1}{(\lambda^2 - 1)(\mu^2 - 1)}. \tag{3.10}$$

Hence it is only at this single value of w that $D_w(p)$ can have multiple zeros at $p = \pm 1$. \square

Under the transformation (3.6), the zeros of $D_w(p)$ are related to the zeros of the orthogonal polynomial $P_w(z)$, which are all real. The transformation from z to p then implies that $D_w(p)$ can only have roots on the unit circle or the real axis. Thus it makes sense to introduce the parametrization $p = e^{it}$ for roots on the unit circle. A straightforward calculation leads to the results summarized in the following lemma.

Lemma 2. *The zeros of the polynomial $D_w(p)$ are given by $p_k = e^{it_k}$, where*

$$\tan wt_k = \frac{\left(\frac{\lambda^2 - 1}{\lambda^2 + 1} + \frac{\mu^2 - 1}{\mu^2 + 1} \right) \tan t_k}{\left(\frac{\lambda^2 - 1}{\lambda^2 + 1} \right) \left(\frac{\mu^2 - 1}{\mu^2 + 1} \right) - \tan^2 t_k}. \tag{3.11}$$

Additionally, for $\lambda = 1$ or $\mu = 1$, $D_w(p) = 0$ at $p = \pm 1$. If $\lambda = \mu = 1$, $p = \pm 1$ is a triple zero of $D_w(p)$. In particular, for w sufficiently large, the numbers of zeros of $D_w(p)$, including their multiplicity, are given as follows:

- (1) If $\lambda < 1$ and $\mu < 1$, equation (3.11) has $2w + 4$ real solutions. $D_w(p)$ has $2w + 4$ zeros on the unit circle.
- (2) On the line segments $\lambda < 1$ and $\mu = 1$, respectively, $\lambda = 1$ and $\mu < 1$, equation (3.11) has $2w + 2$ solutions. $D_w(p)$ has $2w + 4$ zeros on the unit circle.
- (3) If $\lambda = \mu = 1$, equation (3.11) has $2w$ solutions. $D_w(p)$ has $2w + 4$ zeros on the unit circle.
- (4) If $\lambda > 1$ and $\mu < 1$ or $\lambda < 1$ and $\mu > 1$, equation (3.11) has $2w$ solutions. $D_w(p)$ has $2w$ zeros on the unit circle and four zeros on the real line.
- (5) On the line segments $\lambda > 1$ and $\mu = 1$, respectively, $\lambda = 1$ and $\mu > 1$, equation (3.11) has $2w - 2$ solutions. $D_w(p)$ has $2w$ zeros on the unit circle and four zeros on the real line.
- (6) If $\lambda > 1$ and $\mu > 1$, equation (3.11) has $2w - 4$ solutions. $D_w(p)$ has $2w - 4$ zeros on the unit circle and eight zeros on the real line.

This corresponds to $(2w + 4) - 4\sigma$ zeros p_k of $D_w(p)$ on the unit circle, where $\sigma \in \{0, 1, 2\}$, depending on the values of λ and μ . The other 4σ zeros p_k are located on the real line. If p_k is a real zero, then so is $-p_k, 1/p_k$ and $-1/p_k$.

Proof. Equation (3.11) is obtained from $D_w(p)$ by substitution of $p = e^{it}$, followed by routine simplification. The number of real solutions is most easily obtained by considering the graphs of the lhs and rhs of (3.11) over the interval $[0, 2\pi)$. The function $\tan wt_k$ is monotonic and has $2w$ simple poles, whereas the behaviour of the rhs depends on the values of λ and μ . For example, if both $\lambda < 1$ and $\mu < 1$, the rhs is monotonically decreasing and has four poles, leading to a total number of $2w + 4$ intersections of both graphs. The other cases can be obtained similarly. □

Remark. The real roots p_k can be obtained correspondingly from $p_k = e^{s_k}$, where now

$$\tanh ws_k = \frac{\left(\frac{\lambda^2-1}{\lambda^2+1} + \frac{\mu^2-1}{\mu^2+1}\right) \tanh s_k}{\left(\frac{\lambda^2-1}{\lambda^2+1}\right)\left(\frac{\mu^2-1}{\mu^2+1}\right) + \tanh^2 s_k}. \tag{3.12}$$

4. Partition function identities

In this section, we derive explicit expressions for the partition function which are especially suited for an asymptotic analysis of the finite-size scaling behaviour. The key is the following lemma.

Lemma 3.

$$Z_{n,w}(a, b) = -\frac{1}{2} \sum_{p_k} \text{Res}(f; p_k), \tag{4.1}$$

where

$$f(p) = \frac{(1 - p^2)[(1 - \mu^2 p^2) + (\mu^2 - p^2)p^{2w}]}{D_w(p)} \left(\frac{1 + p^2}{p}\right)^n \frac{1}{p} \tag{4.2}$$

and p_k are the zeros of $D_w(p)$.

Proof. From equation (2.8) it follows that

$$Z_{n,w}(a, b) = \frac{1}{2\pi i} \oint f(p) dp, \tag{4.3}$$

with $f(p)$ given in equation (4.2). The integrand is a rational function in p so that the sum over all its residues on the Riemann sphere is equal to zero. From this it follows that

$$Z_{n,w}(a, b) = \text{Res}(f; 0) = - \sum_{p_k} \text{Res}(f; p_k) - \text{Res}(f; \infty), \quad (4.4)$$

where the p_k are the zeros of $D_w(p)$.

Due to the symmetry

$$f(1/p) = -p^2 f(p) \quad (4.5)$$

the singularities p_k come in pairs $(p_k, 1/p_k)$ and the paired residues are equal, i.e.

$$\text{Res}(f; p_k) = \text{Res}(f; 1/p_k). \quad (4.6)$$

It therefore follows that

$$Z_{n,w}(a, b) = \text{Res}(f; 0) = -\frac{1}{2} \sum_{p_k} \text{Res}(f; p_k). \quad (4.7)$$

□

It is convenient to first look at the special cases already considered above (see equation (3.2)).

Proposition 4. *We have*

$$Z_{n,w}(1, 1) = \frac{2^{n+1}}{w+2} \sum_{k=1}^{w+1} \sin^2 \frac{k\pi}{w+2} \cos^n \frac{k\pi}{w+2}, \quad (4.8a)$$

$$Z_{n,w}(1, 2) = \frac{2^n}{w+1} \sum_{k=0}^{2w+1} \sin^2 \frac{(2k+1)\pi}{2w+2} \cos^n \frac{(2k+1)\pi}{2w+2}, \quad (4.8b)$$

$$Z_{n,w}(2, 1) = \frac{2^n}{2(w+1)} \sum_{k=0}^{2w+1} \cos^n \frac{(2k+1)\pi}{2w+2}, \quad (4.8c)$$

$$Z_{n,w}(2, 2) = \frac{2^n}{w} \sum_{k=0}^{w-1} \cos^n \frac{k\pi}{w} \quad (4.8d)$$

and

$$\begin{aligned} Z_{n,w}(1 + \lambda^2, 1 + \lambda^{-2}) &= \frac{1 - \lambda^2}{2\lambda^2} \frac{\lambda^{2w}}{1 - \lambda^{2w}} (\lambda + \lambda^{-1})^n (1 + (-1)^n) \\ &+ \frac{2^n}{\lambda w} \sum_{k=1}^{w-1} \frac{\frac{\lambda + \lambda^{-1}}{2} \sin^2 \frac{k\pi}{w}}{\left(\frac{\lambda - \lambda^{-1}}{2}\right)^2 + \sin^2 \frac{k\pi}{w}} \cos^n \frac{k\pi}{w} \end{aligned} \quad (4.8e)$$

for $\lambda \neq 1$.

Proof. Equation (3.2) allows for an explicit calculation of the zeros of $D_w(p)$. An application of lemma 3 gives the result. □

We note that the expression for $Z_{n,w}(1, 1)$ is a special case of results in [10]. For general values of λ and μ , we arrive at the following result.

Proposition 5. For $\lambda\mu \neq 1$ and w sufficiently large,

$$Z_{n,w}(a, b) = \frac{1 + \lambda^2}{4} \sum_{p_k} \frac{(1 - p_k^2)^2}{(\lambda^2 - p_k^2)(1 - \lambda^2 p_k^2)} \left(\frac{1 + p_k^2}{p_k}\right)^n \frac{1}{w + \varepsilon_k}, \quad (4.9)$$

where p_k are the zeros of $D_w(p)$ and

$$\varepsilon_k = p_k^2 \left[\frac{\lambda^2}{1 - \lambda^2 p_k^2} - \frac{1}{\lambda^2 - p_k^2} + \frac{\mu^2}{1 - \mu^2 p_k^2} - \frac{1}{\mu^2 - p_k^2} \right]. \quad (4.10)$$

Proof. Using lemma 3, we write $f(p) = r(p)/D_w(p)$ with

$$r(p) = (1 - p^2)[(1 - \mu^2 p^2) + (\mu^2 - p^2)p^{2w}] \left(\frac{1 + p^2}{p}\right)^n \frac{1}{p}. \quad (4.11)$$

According to lemma 1, all roots of $D_w(p)$ are simple for w sufficiently large, and $p = \pm 1$ are removable singularities of $f(p)$ due to the occurrence of the factor $(1 - p^2)$ in $r(p)$. Using that

$$\text{Res}(f; p_k) = r(p_k)/D'_w(p_k) \quad (4.12)$$

for simple poles at p_k , we find that

$\text{Res}(f; p_k) =$

$$-\frac{(1 - p_k^2)[(1 - \mu^2 p_k^2) + (\mu^2 - p_k^2)p_k^{2w}]\left(\frac{1 + p_k^2}{p_k}\right)^n}{2w(\lambda^2 - p_k^2)(\mu^2 - p_k^2)p_k^{2w} + 2p_k^2[(\lambda^2 + \mu^2 - 2\lambda^2\mu^2 p_k^2) - (\lambda^2 + \mu^2 - 2p_k^2)p_k^{2w}]}. \quad (4.13)$$

Eliminating p_k^{2w} using $D_w(p_k) = 0$ gives

$$\text{Res}(f; p_k) = -\frac{1 + \lambda^2}{2} \frac{(1 - p_k^2)^2}{(\lambda^2 - p_k^2)(1 - \lambda^2 p_k^2)} \left(\frac{1 + p_k^2}{p_k}\right)^n \frac{1}{w + \varepsilon_k}, \quad (4.14)$$

where ε_k is given by (4.10). □

Remark. The condition $\lambda\mu \neq 1$ is necessary because when $\lambda\mu = 1$ a root, p_k , is located at $p_k = \lambda$, making the expression for $Z_{n,w}(a, b)$ invalid as is written. However, in this case we already have given a much more explicit expression for $Z_{n,w}(a, b)$ above.

5. Asymptotics

If we consider the scaling behaviour of long walks in wide strips, the behaviour of our model should depend on the relation between average vertical displacement of an unrestricted polymer and the width of the strip, w . We therefore expect the occurrence of the scaling combination \sqrt{n}/w in the asymptotics, and this is indeed what a mathematical analysis shows.

As in the previous sections, it is convenient to first consider the special cases.

Proposition 6. For n even, \sqrt{n}/w fixed and $n \rightarrow \infty$,

$$Z_{n,w}(1, 1) \sim \frac{2^n}{n^{3/2}} f_{0,0}(\sqrt{n}/w), \quad (5.1a)$$

$$Z_{n,w}(1, 2) \sim \frac{2^n}{n^{3/2}} f_{0,1}(\sqrt{n}/w), \quad (5.1b)$$

$$Z_{n,w}(2, 1) \sim \frac{2^n}{n^{1/2}} f_{1,0}(\sqrt{n}/w), \tag{5.1c}$$

$$Z_{n,w}(2, 2) \sim \frac{2^n}{n^{1/2}} f_{1,1}(\sqrt{n}/w), \tag{5.1d}$$

for $\lambda < 1$ we have

$$Z_{n,w}(1 + \lambda^2, 1 + \lambda^{-2}) \sim \frac{1 - \lambda^2}{\lambda^2} \lambda^{2w} (\lambda + \lambda^{-1})^n + \frac{2^n}{n^{3/2}} f_{\lambda,\lambda^{-1}}(\sqrt{n}/w), \tag{5.1e}$$

while for $\lambda > 1$ we have

$$Z_{n,w}(1 + \lambda^2, 1 + \lambda^{-2}) \sim \frac{\lambda^2 - 1}{\lambda^2} (\lambda + \lambda^{-1})^n + \frac{2^n}{n^{3/2}} f_{\lambda,\lambda^{-1}}(\sqrt{n}/w). \tag{5.1f}$$

The functions $f_{\lambda,\mu}$ are given by

$$f_{0,0}(x) = 2\pi^2 x^3 \sum_{k=-\infty}^{\infty} k^2 e^{-\frac{\pi^2 k^2}{2} x^2} = 2\pi^2 x^3 e^{-\frac{\pi^2 x^2}{2}} \vartheta_3'(e^{-\frac{\pi^2 x^2}{2}}), \tag{5.2a}$$

$$f_{0,1}(x) = 2\pi^2 x^3 \sum_{k=-\infty}^{\infty} (k + 1/2)^2 e^{-\frac{\pi^2 (k+1/2)^2}{2} x^2} = 2\pi^2 x^3 e^{-\frac{\pi^2 x^2}{2}} \vartheta_2'(e^{-\frac{\pi^2 x^2}{2}}), \tag{5.2b}$$

$$f_{1,0}(x) = x \sum_{k=-\infty}^{\infty} e^{-\frac{\pi^2 (k+1/2)^2}{2} x^2} = x \vartheta_2(e^{-\frac{\pi^2 x^2}{2}}), \tag{5.2c}$$

$$f_{1,1}(x) = x \sum_{k=-\infty}^{\infty} e^{-\frac{\pi^2 k^2}{2} x^2} = x \vartheta_3(e^{-\frac{\pi^2 x^2}{2}}), \tag{5.2d}$$

for $\lambda \neq 1$,

$$f_{\lambda,\lambda^{-1}}(x) = \frac{(\lambda^2 + 1)}{(\lambda^2 - 1)^2} 2\pi^2 x^3 \sum_{k=0}^{\infty} k^2 e^{-\frac{\pi^2 k^2}{2} x^2} = \frac{(\lambda^2 + 1)}{(\lambda^2 - 1)^2} 2\pi^2 x^3 e^{-\frac{\pi^2 x^2}{2}} \vartheta_3'(e^{-\frac{\pi^2 x^2}{2}}). \tag{5.2e}$$

Here, $\vartheta_2(q) = \sum_{n=-\infty}^{\infty} q^{(n+1/2)^2}$ and $\vartheta_3(q) = \sum_{n=-\infty}^{\infty} q^{n^2}$ are elliptic ϑ functions.

Proof. We shall only discuss the case $\lambda = \mu = 1$, as the argument applies *mutatis mutandum* to the other cases. Upon introducing the variable $x = n^{1/2}/w$, we can write

$$Z_{n,w}(2, 2) = \frac{2^n x}{n^{1/2}} \sum_{k=0}^{w-1} \cos^n \left(\frac{k\pi x}{n^{1/2}} \right). \tag{5.3}$$

For fixed k we find that

$$\lim_{n \rightarrow \infty} \cos^n \left(\frac{k\pi x}{n^{1/2}} \right) = e^{-\frac{\pi^2 k^2}{2} x^2}, \tag{5.4}$$

and a similar contribution comes from the upper boundary of the summation for $k' = w - k$ fixed. The contribution to the sum from other terms can be easily shown to be negligible, so that

$$\lim_{n \rightarrow \infty} \frac{n^{1/2}}{2^n} Z_{n,(n^{1/2}/x)}(2, 2) = x \sum_{k=-\infty}^{\infty} e^{-\frac{\pi^2 k^2}{2} x^2}. \tag{5.5}$$

□

In figure 4, we have plotted the scaling functions at the points $\lambda, \mu \in \{0, 1\}$. These show that the partition functions converge rapidly to the scaling functions even at quite modest

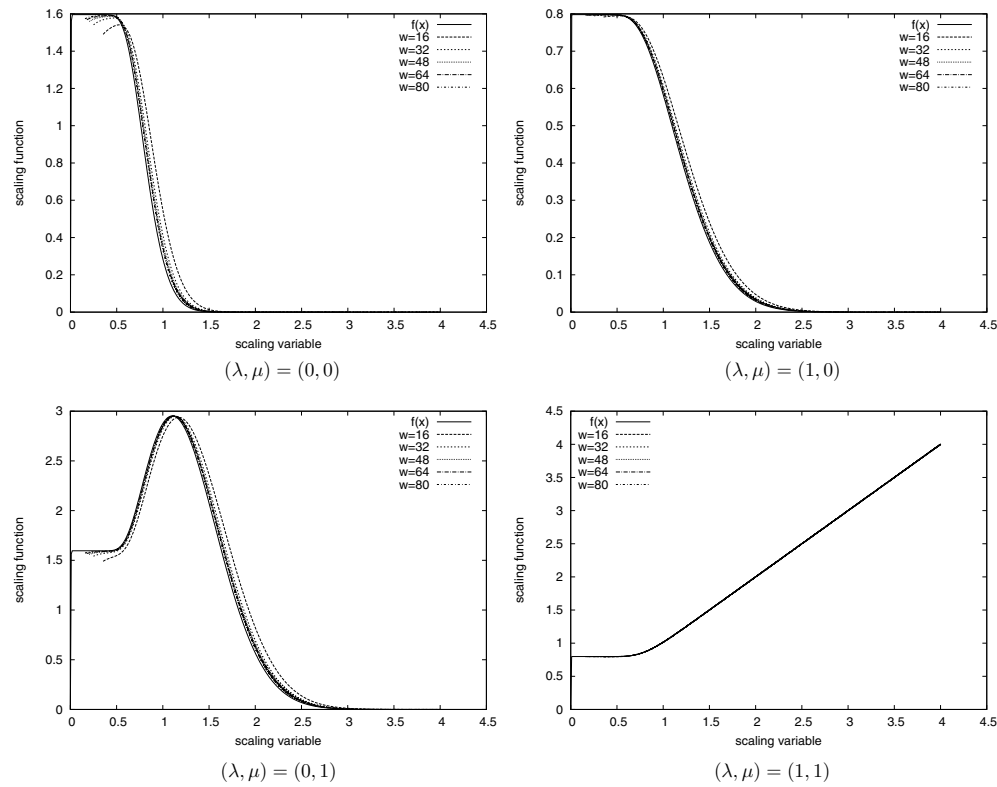


Figure 4. The scaling functions (solid lines) at $(\lambda, \mu) = (0, 0), (1, 0), (0, 1)$ and $(1, 1)$, respectively. Also plotted is numerical data (dashed lines) for widths ranging from 16 to 80; these show that the partition functions converge rapidly to the scaling forms.

widths (w ranges from 16 to 80 and the maximum length is $16w^2$). The non-monotonic behaviour of $f_{01}(x)$ has also been observed in the three-dimensional self-avoiding walk model at a comparable point in the phase diagram [4].

Remark. We note that even though we have only considered the scaling limit of $x = \sqrt{n}/w$ fixed, the above scaling forms permit asymptotic matching to the limits $w \rightarrow \infty$ with n fixed, and $n \rightarrow \infty$ with w fixed. For example, we obtain

$$\frac{2^n}{n^{1/2}} f_{1,1}(\sqrt{n}/w) \sim \begin{cases} \frac{1}{w} 2^n & n \rightarrow \infty \\ \sqrt{\frac{2}{\pi n}} 2^n & w \rightarrow \infty \end{cases} \quad (5.6)$$

which agrees with the known asymptotic behaviour of $Z_{n,w}(2, 2)$ for fixed w or n , respectively.

In order to discuss the case of general a and b , let us consider equation (4.9) more closely. Note that for large w the terms ε_k given by (4.10) become negligible in comparison with w if p_k is a root on the unit circle, as ε_k is then uniformly bounded in k , w and n . Also note that in this case the dependence of (4.9) on μ enters only through the roots p_k .

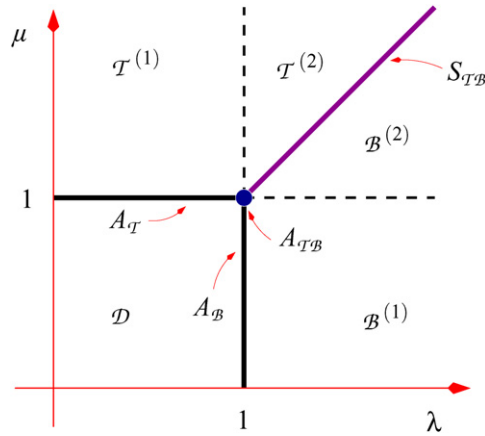


Figure 5. Regions that have different scaling forms. The definitions via inequalities occur in equation (5.14). The region $T^{(1)}$ includes the dashed line segment $\lambda = 1, \mu > 1$ and the region $B^{(1)}$ includes the dashed line segment $\mu = 1, \lambda > 1$.

However, if p_k is a real root it needs to be treated individually, and we therefore split the partition function into two sums,

$$Z_{n,w}(a, b) = Z_{n,w}^{(e)}(a, b) + Z_{n,w}^{(s)}(a, b), \tag{5.7}$$

where

$$Z_{n,w}^{(e)}(a, b) = \frac{1 + \lambda^2}{4} \sum_{|p_k| \neq 1} \frac{(1 - p_k^2)^2}{(\lambda^2 - p_k^2)(1 - \lambda^2 p_k^2)} \left(\frac{1 + p_k^2}{p_k} \right)^n \frac{1}{w + \varepsilon_k} \tag{5.8}$$

and

$$Z_{n,w}^{(s)}(a, b) = \frac{1 + \lambda^2}{4} \sum_{|p_k|=1} \frac{(1 - p_k^2)^2}{(\lambda^2 - p_k^2)(1 - \lambda^2 p_k^2)} \left(\frac{1 + p_k^2}{p_k} \right)^n \frac{1}{w + \varepsilon_k}. \tag{5.9}$$

Here, $Z_{n,w}^{(e)}(a, b)$ is a sum over zero, four or eight terms, depending on the value of w, λ and μ . While it turns out that $Z_{n,w}^{(s)}(a, b)$ admits a scaling form, $Z_{n,w}^{(e)}(a, b)$ does not. The following propositions give asymptotic estimates for $Z_{n,w}^{(e)}(a, b)$ and $Z_{n,w}^{(s)}(a, b)$ for large w .

The analysis of $Z_{n,w}^{(e)}(a, b)$ uses an asymptotic estimate of the zeros for which $p_k > 1$, analogous to equations (7.7) and (7.10) in [2]. If $\lambda > 1$ and $\mu \neq \lambda$, we find

$$p^2 \sim \lambda^2 + (\lambda^4 - 1) \left(\frac{\lambda^2 \mu^2 - 1}{\lambda^2 - \mu^2} \right) \lambda^{-2w}, \tag{5.10}$$

and if $\mu > 1$ and $\lambda \neq \mu$, we find

$$p^2 \sim \mu^2 + (\mu^4 - 1) \left(\frac{\lambda^2 \mu^2 - 1}{\mu^2 - \lambda^2} \right) \mu^{-2w}, \tag{5.11}$$

while for $\lambda = \mu > 1$, we find

$$p^2 \sim \lambda^2 \pm (\lambda^4 - 1) \lambda^{-w}. \tag{5.12}$$

In figure 5 we introduce a finer division of the regions of the phase plane which will be needed below; essentially we split the regions T and B into two parts.

From the considerations above, we arrive at the following result.

Proposition 7. For n even and $n \rightarrow \infty$,

$$Z_{n,w}^{(e)}(a, b) \sim \begin{cases} \left[\frac{(\lambda^2 + 1)(\mu^2 - 1)^2(\mu^4 - 1)}{\mu^2(\mu^2 - \lambda^2)^2} \mu^{-2w} (\mu + \mu^{-1})^n \right] & \text{in the region } \mathcal{T}^{(1)}, \\ \left[\frac{(\lambda^2 + 1)(\mu^2 - 1)^2(\mu^4 - 1)}{\mu^2(\mu^2 - \lambda^2)^2} \mu^{-2w} (\mu + \mu^{-1})^n + \frac{\lambda^2 - 1}{\lambda^2} (\lambda + \lambda^{-1})^n \right] & \text{in the region } \mathcal{T}^{(2)}, \\ \frac{\lambda^2 - 1}{\lambda^2} (\lambda + \lambda^{-1})^n & \text{on the line } S_{TB}, \\ \left[\frac{\lambda^2 - 1}{\lambda^2} (\lambda + \lambda^{-1})^n + \frac{(\lambda^2 + 1)(\mu^2 - 1)^2(\mu^4 - 1)}{\mu^2(\mu^2 - \lambda^2)^2} \mu^{-2w} (\mu + \mu^{-1})^n \right] & \text{in the region } \mathcal{B}^{(2)}, \text{ and} \\ \frac{\lambda^2 - 1}{\lambda^2} (\lambda + \lambda^{-1})^n & \text{in the region } \mathcal{B}^{(1)}, \end{cases} \quad (5.13)$$

where

$$\begin{aligned} S_{TB} &= \{(\mu, \lambda) | \mu = \lambda > 1\}, \\ \mathcal{T}^{(1)} &= \{(\mu, \lambda) | \mu > 1 \geq \lambda\}, & \mathcal{T}^{(2)} &= \{(\mu, \lambda) | \mu > \lambda > 1\}, \\ \mathcal{B}^{(1)} &= \{(\mu, \lambda) | \lambda > 1 \geq \mu\}, & \mathcal{B}^{(2)} &= \{(\mu, \lambda) | \lambda > \mu > 1\}. \end{aligned} \quad (5.14)$$

The asymptotic estimate for $Z_{n,w}^{(s)}(a, b)$ is done in two stages. First, we present an estimate for large w which is uniform in n .

Proposition 8.

$$Z_{n,w}^{(s)}(a, b) = \left(\frac{\lambda + \lambda^{-1}}{4\lambda} \right) \frac{2^n}{w} \sum_{t_k} \left(\frac{\sin^2 t_k}{\left(\frac{\lambda - \lambda^{-1}}{2}\right)^2 + \sin^2 t_k} \cos^n t_k \right) [1 + O(w^{-1})] \quad (5.15)$$

uniformly in n , where t_k are the roots of (3.11) in $[0, \pi)$.

Proof. Apart from substituting $p_k = e^{it_k}$ and simplifying, the main effort lies in obtaining an estimate for ε_k . For $\lambda, \mu \neq 1$, we can estimate it directly from (4.10)

$$|\varepsilon_k| < \frac{\lambda^2 + 1}{|\lambda^2 - 1|} + \frac{\mu^2 + 1}{|\mu^2 - 1|}. \quad (5.16)$$

If $\lambda = 1$, we find that

$$|\varepsilon_k| < \frac{\mu^2 + 1}{|\mu^2 - 1|}, \quad (5.17)$$

and analogously for $\mu = 1$. Finally, if both $\lambda = 1$ and $\mu = 1$ then $\varepsilon_k = 0$. □

For the scaling behaviour of $Z_{n,w}^{(s)}(a, b)$, we find identical scaling behaviour as in the special cases discussed above (except for λ -dependent pre-factors).

Proposition 9. For n even, \sqrt{n}/w fixed and $n \rightarrow \infty$,

$$Z_{n,w}^{(s)}(a, b) \sim \begin{cases} \frac{2^n}{n^{3/2}} f(\sqrt{n}/w) & \text{for } \lambda \neq 1, \\ \frac{2^n}{n^{1/2}} f(\sqrt{n}/w) & \text{for } \lambda = 1, \end{cases} \quad (5.18)$$

where

$$f(x) = \begin{cases} x\vartheta_3\left(e^{-\frac{\pi^2 x^2}{2}}\right) & \text{for } \lambda = 1 \text{ and } \mu = 1, \\ \frac{\lambda^2 + 1}{(\lambda^2 - 1)^2} 2\pi^2 x^3 e^{-\frac{\pi^2 x^2}{2}} \vartheta_2'\left(e^{-\frac{\pi^2 x^2}{2}}\right) & \text{for } \lambda \neq 1 \text{ and } \mu = 1, \\ x\vartheta_2\left(e^{-\frac{\pi^2 x^2}{2}}\right) & \text{for } \lambda = 1 \text{ and } \mu \neq 1, \text{ and} \\ \frac{\lambda^2 + 1}{(\lambda^2 - 1)^2} 2\pi^2 x^3 e^{-\frac{\pi^2 x^2}{2}} \vartheta_3'\left(e^{-\frac{\pi^2 x^2}{2}}\right) & \text{for } \lambda \neq 1 \text{ and } \mu \neq 1. \end{cases} \quad (5.19)$$

Here, $\vartheta_2(q) = \sum_{n=-\infty}^{\infty} q^{(n+1/2)^2}$ and $\vartheta_3(q) = \sum_{n=-\infty}^{\infty} q^{n^2}$ are elliptic ϑ functions.

Proof. The derivation is done in complete analogy to the special cases discussed above. The only additional consideration is that now t_k is only known asymptotically for w large. If either $\lambda \neq 1$ and $\mu \neq 1$ or $\lambda = \mu = 1$, then for large w we find

$$t_k \sim k \frac{\pi}{w} \quad (5.20)$$

and otherwise (i.e. if $\lambda = 1$ or $\mu = 1$ but not $\lambda = \mu = 1$) for large w we find

$$t_k \sim (k + 1/2) \frac{\pi}{w}. \quad (5.21)$$

□

We point out that these functions, which are effectively multiples of the scaling functions (see below), are elliptic ϑ functions. Further they are independent of λ and μ , apart from that overall multiplicative factor, which is dependent only on λ (as it depends on the half-plane limit). Finally, we note that the result for $\lambda = \mu = 0$ is equivalent to asymptotic results of Flajolet *et al* [11] concerning the distribution of heights of binary trees since there is a correspondence between directed paths and binary trees.

6. Discussion

We now return to the issue of how the scaling forms calculated above interpolate between the half plane and the infinite slit. For the half plane, we have (recalling $a = 1 + \lambda^2$ and $b = 1 + \mu^2$)

$$Z_n^{hp}(a) = \lim_{w \rightarrow \infty} Z_{n,w}(a, b) \sim \begin{cases} \left[\frac{2(1 + \lambda^2)}{(1 - \lambda^2)^2} \sqrt{\frac{2}{\pi}} \right] \frac{2^n}{n^{3/2}} & 0 \leq a < 2 (0 \leq \lambda < 1), \\ \left[\sqrt{\frac{2}{\pi}} \right] \frac{2^n}{n^{1/2}} & a = 2 (\lambda = 1), \\ \left[\frac{(\lambda^2 - 1)}{\lambda^2} \right] (\lambda + \lambda^{-1})^n & a > 2 (\lambda > 1), \end{cases} \quad (6.1)$$

as $n \rightarrow \infty$. Note that the scaling is independent of b , as it should be for $w > n$. For any finite w , we expect that

$$Z_{n,w}(a, b) \sim B_w(a, b) \mu_w(a, b)^n, \quad (6.2)$$

where as $w \rightarrow \infty$ we have

$$\mu_w(a, b) \rightarrow \begin{cases} 2 & 0 \leq a, \quad b \leq 2, \\ (\lambda + \lambda^{-1}) & a \geq b \quad \text{and} \quad a > 2, \\ (\mu + \mu^{-1}) & a < b \quad \text{and} \quad b > 2. \end{cases} \quad (6.3)$$

If we denote the right-hand side of equation (6.1) as $S^{hp}(n)$ for each value of a then a canonical general scaling ansatz is

$$Z_{n,w}(a, b) \sim S^{hp}(n) f_{\text{phase}} \left(\frac{n^{\nu_{\perp}}}{w} \right). \tag{6.4}$$

The scaling function f_{phase} depends on which phase or phase boundary of the infinite slit the values of a and b correspond (so as to match with the infinite slit phases). The exponent ν_{\perp} , on the other hand, should depend on the phase of the half-plane problem.

We immediately note that there is something unusual here and that while ν_{\perp} is expected to be $1/2$ for $0 \leq a \leq 2$ it is expected to be 0 for $a > 2$! In Martin *et al* [4], it was proposed that a scaling theory like that in equation (6.4) (see equations (3.5)–(3.7) of that paper) should only hold in the desorbed region of the infinite slit or on its boundaries. That is, we should expect a scaling theory only when $0 \leq a, b \leq 2$ —this is precisely when $\nu_{\perp} = 1/2 > 0$. This is what we have found for the directed walk case.

Now, to *match* the scaling in equation (6.1) (half-plane matching) one would require that

$$f_{\text{phase}}(x) \sim 1 \quad \text{as} \quad x \rightarrow 0. \tag{6.5}$$

This is a similar requirement to that of equation (3.6) of Martin *et al* [4]. On the other hand, the scaling of f_{phase} as $x \rightarrow \infty$ needs to be considered in order to match the scaling of the *infinite slit* (equations (6.2) and (6.3)).

Our results show that the partition function $Z_{n,w}(a, b)$ can be found as two parts $Z^{(e)}$ and $Z^{(s)}$ as given in equations (5.13) and (5.18), respectively. Importantly, for $0 \leq a, b \leq 2$ we have $Z^{(e)} = 0$ and the form (5.18) for $Z^{(s)}$ is precisely that of (6.4) with the half-plane matching behaviour (6.5) obeyed by (5.19). The functions (5.19) also obey the required *infinite-slit* matching behaviour; that is,

$$f_{\text{phase}}(x) \propto \begin{cases} x & \text{for } a = b = 2, \\ x^3 e^{-\pi^2 x^2/8} & \text{for } a < 2 \text{ and } b = 2, \\ x e^{-\pi^2 x^2/8} & \text{for } a = 2 \text{ and } b < 2, \text{ and} \\ x^3 e^{-\pi^2 x^2/2} & \text{for } a < 2 \text{ and } b < 2, \end{cases} \tag{6.6}$$

as $x \rightarrow \infty$. This large x behaviour allows for the recovery of (6.2) with (6.3). They also give us the first correction to the free energy as a function of w (see equations (7.3) and (7.6) of Brak *et al* [2]). From equation (3.7) of Martin *et al* [4] we find that the above results also agree with that generic prediction.

For any value of (a, b) such that either $a > 2$ and/or $b > 2$, $Z^{(e)} \neq 0$ and furthermore $Z^{(e)} \gg Z^{(s)}$ as $n \rightarrow \infty$. As far as we can calculate, $Z^{(e)}$ cannot be written in the scaling function form (6.4). We note that the scaling form of $Z^{(s)}$ acts as a correction to scaling to that of $Z^{(e)}$ which allows for a *matching* of the total form $Z^{(e)} + Z^{(s)}$ with the half-plane and infinite-slit limits. Since the dominant part of the form of $Z^{(e)}$ in (5.13) is that of (6.2) with the connective constant as in (6.3) the infinite-slit behaviour is clearly adhered to (although the coefficient $B_w(a, b)$ may go to zero in this limit).

Consider equation (5.13). For $b > 2$ and $a \leq 2$ (region $\mathcal{T}^{(1)}$) $Z^{(e)} \sim \mu^{-2w} \rightarrow 0$ as $w \rightarrow \infty$ (n fixed and large) so for the half plane one is left with $Z^{(s)}$ with $x \rightarrow 0$. For $a > 2$ and $b \leq 2$ (region $\mathcal{B}^{(1)}$), the scaling form in (5.13) coincides with that of (6.1) for $a > 2$ so that the half-plane limit is simple. For $a = b > 2$ (line $\mathcal{S}_{\mathcal{T}\mathcal{B}}$) this is also true. For $a > 2$ and $b > 2$ with $a \neq b$ (regions $\mathcal{T}^{(2)}$ and $\mathcal{B}^{(2)}$), there are two parts of the scaling form of $Z^{(e)}$ with one part going to zero for $w \rightarrow \infty$ leaving the appropriate scaling corresponding to the half plane.

The above shows how complicated, though mathematically complete, the scaling picture can be for this problem. To summarize, we have calculated the scaling for large widths and

large lengths of directed walks confined between the two walls that interact with the walk. We explicitly demonstrate that the conjectured scaling theory [4] for polymers confined in such a manner holds exactly for this model. This theory holds when the polymer is in a desorbed state, or on the boundaries of this region in the parameter space, that is critically adsorbing.

Acknowledgments

Financial support from NSERC of Canada, the Australian Research Council and the Centre of Excellence for Mathematics and Statistics of Complex Systems is gratefully acknowledged by the authors.

References

- [1] DiMarzio E A and Rubin R J 1971 *J. Chem. Phys.* **55** 4318–36
- [2] Brak R, Owczarek A L, Rechnitzer A and Whittington S 2005 *J. Phys. A: Math. Gen.* **38** 4309–25
- [3] Janse van Rensburg E J, Orlandini E, Owczarek A L, Rechnitzer A and Whittington S G 2005 *J. Phys. A: Math. Gen.* **38** L823–8
- [4] Martin R, Orlandini E, Owczarek A L, Rechnitzer A and Whittington S G 2007 *J. Phys. A: Math. Gen.* **40** 7509–21
- [5] Janse van Rensburg E J, Orlandini E and Whittington S 2006 *J. Phys. A: Math. Gen.* **39** 13869
- [6] Brak R, Essam J, Osborn J, Owczarek A L and Rechnitzer A 2006 *J. Phys.: Conf. Ser.* **42** 47–58
- [7] Geronimus Ja L 1977 Orthogonal polynomials *Am. Math. Soc. Transl. Ser. 2* **108** 37–130
- [8] Chihara T S An introduction to orthogonal polynomials *Math. Appl.* **13** 1978
- [9] Andrews G E, Askey R and Roy R 1999 Special functions *Encyclopedia of Mathematics and its Applications* (Cambridge: Cambridge University Press)
- [10] Krattenthaler C, Guttmann A J and Viennot X G 2003 *J. Stat. Phys.* **110** 1069–86
- [11] Flajolet P, Gao Z, Odlyzko A and Richmond B 1993 *Comb. Probab. Comput.* **2** 145–56